17

Non-Volatile Resistive Switching in Graphene Oxide Thin Films

Fei Zhuge, Run-Wei Li,* Congli He, Zhaoping Liu and Xufeng Zhou
Ningbo Institute of Materials Technology and Engineering,
Chinese Academy of Sciences,
People's Republic of China

1. Introduction

The semiconductor industry has long been seeking a high-density, high-speed, and low-power memory technology that retains its data even when the power is interrupted (Meijer, 2008). Though static random access memory (SRAM) and dynamic random access memory (DRAM) are very fast, both of them are volatile, which is a huge disadvantage, costing energy and additional periphery circuitry. Si-based Flash memory devices represent the most prominent nonvolatile data memory (NVM) because of their high density and low fabrication costs. However, Flash suffers from low endurance, low write speed, and high voltages required for the write operations. In addition, further scaling, i.e., a continuation in increasing the density of Flash is expected to run into physical limits in the near future. Ferroelectric random access memory (FeRAM) and magnetoresistive random access memory (MRAM) cover niche markets for special applications. One reason among several others is that FeRAM as well as conventional MRAM exhibit technological and inherent problems in the scalability, i.e., in achieving the same density as Flash today. In this circumstance, a renewed nonvolatile memory concept called resistance-switching random access memory (RRAM), which is based on resistance change modulated by electrical stimulus, has recently inspired scientific and commercial interests due to its high operation speed, high scalability, and multibit storage potential (Beck et al., 2000; Lu & Lieber, 2007; Dong et al., 2008). The reading of resistance states is nondestructive, and the memory devices can be operated without transistors in every cell (Lee et al., 2007; Waser & Aono, 2007), thus making a cross-bar structure feasible. A large variety of solid-state materials have been found to show these resistive switching characteristics, including solid electrolytes such as GeSe and Ag_2S (Waser & Aono, 2007), perovskites such as $SrZrO_3$ (Beck et al., 2000), $Pr_{0.7}Ca_{0.3}MnO_3$ (Liu et al., 2000; Odagawa et al., 2004; Liao et al., 2009), and $BiFeO_3$ (Yang et al., 2009; Yin et al., 2010; Li et al., 2010), binary transition metal oxides such as NiO (Seo et al., 2004; Kim et al., 2006; Son & Shin, 2008), TiO_2 (Kim et al., 2007; Jeong et al., 2009; Kwon et al., 2010), ZrO_2 (Wu et al., 2007; Guan et al., 2008; Liu et al., 2009), and ZnO (Chang et al., 2008; Kim et al., 2009; Yang et al., 2009), organic materials (Stewart et al., 2004), amorphous silicon (a-Si) (Jo and Lu, 2008; Jo et al., 2009), and amorphous carbon (a-C) (Sinitskii & Tour, 2009; Zhuge et al., 2010).

In last decades, carbon-based materials have been studied intensively as a potential candidate to overcome the scientific and technological limitations of traditional

semiconductor devices (Rueckes et al., 2000; Novoselov et al., 2004; Avouris et al., 2007). It is worthy mentioning that most of the work on carbon-based electronic devices has been focused on field-effect transistors (Wang et al., 2008; Burghard et al., 2009). Thus, it would be of great interest if nonvolatile memory can also be realized in carbon so that logic and memory devices can be integrated on a same carbon-based platform. Graphene oxide (GO) with an ultrathin thickness (~1 nm) is attractive due to its unique physical-chemical properties. A GO layer can be considered as a graphene sheet with epoxide, hydroxyl, and/or carboxyl groups attached to both sides. GO can be readily obtained through oxidizing graphite in mixtures of strong oxidants, followed by an exfoliation process. Due to its water solubility, GO can be transferred onto any substrates uniformly using simple methods such as drop-casting, spin coating, Langmuir-Blodgett (LB) deposition and vacuum filtration. The as-deposited GO thin films can be further processed into functional devices using standard lithography processes without degrading the film properties (Eda et al., 2008; Cote et al., 2009). Furthermore, the band structure and electronic properties of GO can be modulated by changing the quantity of chemical functionalities attached to the surface. Therefore, GO is potentially useful for microelectronics production. Considering that although a large variety of solid-state materials have been found to show resistive switching characteristics, none of them can fully meet the requirements of RRAM applications, exploration of new storage media is still a key project for the development of RRAM. Therefore, in this chapter, the resistive switching effect in GO thin films has been investigated and the possibility of GO used as a potential storage medium for RRAM has been discussed.

2. Experiments

The oxidation of graphite was carried out following the Hummer's method (Hummers & Offeman, 1958). In a typical procedure, KNO_3 (1.2 g) and graphite (1.0 g) was added into 46 mL of concentrated H_2SO_4 (98%) under stirring. After 10 mins 6.0 g of $KMnO_4$ was added slowly. The mixture was then heated to 35 °C and stirred for 6 hours. Subsequently, 80 mL of water was added dropwise under vigorous stirring, resulting in a quick rise of the temperature to ~80 °C. The slurry was further stirred at this temperature for another 30 mins. Afterwards 200 mL of water and 6 mL of H_2O_2 solution were added in sequence to dissolve insoluble manganese species. The resulting graphite oxide suspension was washed repeatedly by a large amount of water until the solution pH reached a constant value at ~4.0, and finally the suspension was diluted to 600 mL with water. 200 mL of the diluted graphite oxide suspension was transferred into a conical beaker with a volume of 500 mL. Then the suspension was gently shaken in a mechanical shaker at a speed of 160 rpm for ~6 hours. To remove the small amount of unexfoliated particles, the resulting viscous suspension was centrifuged at 2,000 rpm for 10 mins, producing a brown, homogeneous colloidal suspension of GO sheets. The colloidal suspension could be further concentrated by centrifugation at 8,000 rpm. Then GO thin films of ~30 nm in thickness were prepared at room temperature by the vacuum filtration method. 50 g of GO suspension with a concentration of 6 mg/L was filtered through a cellulose ester membrane to achieve uniform GO thin films. The film thickness could be well controlled by tuning the GO concentration or filtration volume. The as-filtered GO flakes were then transferred from the filter membrane onto commercial $Pt/Ti/SiO_2/Si$ substrates.

Atomic force microscopy (AFM) characterization was conducted by a Veeco Dimension 3100V scanning probe microscope at ambient conditions using a tapping or conductive-

AFM (CAFM) mode. Scanning electron microscopy (SEM) images were taken by a Hitachi S-4800 Field Emission Scanning Electron Microscope. Specially, a low accelerating voltage of 1.0 kV and high current of 20 μA were applied for the graphene oxide sheets on silicon substrates. In order to measure the electrical properties, metal (Cu, Ag, and Au etc.) top electrodes with a thickness of 200 nm and diameter of 100 μm were deposited at room temperature by electron beam evaporation with an in-situ metal shadow mask. The *I-V* characteristics of metal/GO/Pt structures were measured at room temperature by Keithley 4200 semiconductor characterization system with voltage sweeping mode. During the measurement, a bias voltage was applied between the top (Cu, Ag, and Au etc.) and bottom (Pt) electrodes with the latter being grounded. The schematic structure of the sandwiched devices is depicted in Fig. 1(a). In the local leakage current measurement by CAFM, the conductive tip was grounded and directly touched the GO films, as shown in Fig. 1(b). The resistances in the low resistance state and high resistance state of the metal/GO/Pt structures were measured as a function of temperature by a physical property measurement system (PPMS, Quantum Design).

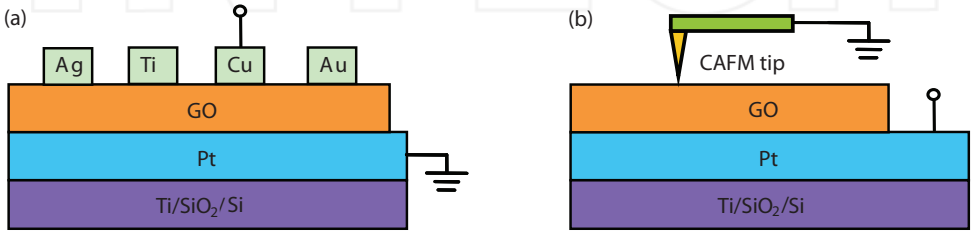

Fig. 1. Schematic configuration (a) of the metal/GO/Pt sandwiched structures, and (b) for the conductive-AFM measurements.

3. Results and discussions

3.1 Morphology of GO sheets and thin films

A typical SEM image of the GO sheets is shown in Fig. 2(a). As can be seen, the sheets have a lateral size, dominantly, in the order of 100 μm, and some of them even possess a size as large as 200 μm. To the best of our knowledge, there have been no reports on GO sheets with such a huge size. Besides the large sheets, fragments with sizes of only a few micrometres can also be observed in a small amount. These fragments might be derived from micrometre-sized graphite flakes or by inevitable breakage during the delamination process. Figure 2(b) displays an AFM image of a GO sheet which has a size far beyond the AFM scan range. The height profile denoted in Fig. 2(b) demonstrates a mean thickness of ~1 nm, indicative of a unilamellar nature of the sheet. It is worth mentioning that the sizes of the exfoliated GO sheets are closely associated with those of the starting graphite flakes. For example, if the graphite flakes of 500 mesh size (~25 μm in mean size) were used, the exfoliated GO sheets had a lateral size around 15 μm. This result indicates that the sheet sizes can be easily controlled through the size selection of the graphite material. Figure 2(c) shows an AFM image of a GO thin film of ~30 nm in thickness deposited at room temperature by the vacuum filtration method. From Fig. 2(c), we see that the as-grown GO film is not smooth and there are a large amount of protuberances on the film surface. These observed protuberances are most likely to be the gauffers of GO sheets formed during the film preparation process (Zhou & Liu, 2010).

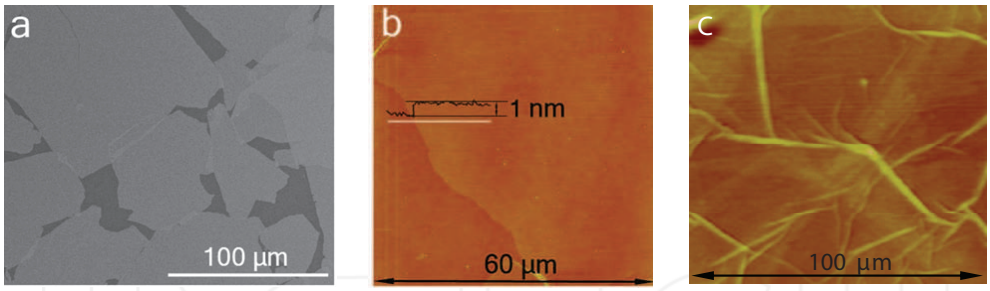

Fig. 2. (a) SEM and (b) AFM images of GO sheets that were deposited on a Si substrate by Langmuir-Blodgett assembly at a constant surface pressure of 10 mN m^{-1}. (c) AFM image of GO thin films of ~30 nm in thickness prepared at room temperature by the vacuum filtration method

3.2 Nonvolatile resistive switching in GO thin films

Metal/GO/Pt sandwiched structures show the bipolar resistive switching behavior (He et al., 2009). The *I-V* characteristics of the Cu/GO/Pt memory cell are studied by dc voltage sweep measurements to evaluate the memory effects of the obtained devices. Figure 3(a) plots a typical *I-V* curve of a Cu/GO/Pt cell. Figure 3(b) shows the same *I-V* curve in a semilogarithmic scale. During the measurement, the voltage is swept in a sequence of 0 V → 1 V → 0 V → –1 V → 0 V with a sweeping step of 0.01 V. While increasing the positive voltage steadily, the current jumps abruptly at a voltage value of about 0.8 V. The device switches from the high resistance state (HRS or Off state) to a low resistance state (LRS or On state), which is called the "Set" process. A current compliance (10 mA in this work) is usually needed during the Set process to prevent the sample from a permanent breakdown. By sweeping the voltage from 1 V to –0.4 V, the device holds on the LRS, and starts switching from the LRS to the HRS ("Reset" process) from –0.4 V. At the voltage of –0.75 V, the cell recovers to the HRS, and holds until next Set process. The *I-V* characteristics exhibit a typical bipolar switching behavior. The device yield of the Cu/GO/Pt structure is more than 50%.

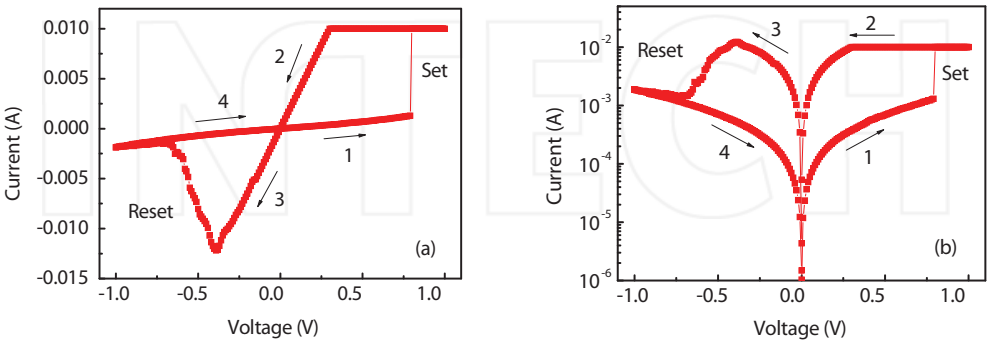

Fig. 3. Typical *I-V* characteristics of the Cu/GO/Pt sandwiched structure shown in (a) linear scale, and (b) semilogarithmic scale. The voltage is swept in the direction as follows: 0 V → 1 V → 0 V → –1 V → 0 V

In order to investigate the endurance performance of the Cu/GO/Pt memory device, cyclic switching operations are conducted. Figure 4(a) shows the evolution of resistance of the two well-resolved states in 100 cycles. The statistical distribution of the resistances in HRS and LRS is shown in Fig. 4(b). The resistance values are read out at –0.1 V in each dc sweep. Although the resistance values of both HRS and LRS show some fluctuations, the On/Off ratios are about 20 without any obvious degradation within 100 cycles. The endurance measurements ensured that the switching between On and Off states is controllable, reversible, and reproducible. After the device was switched On or Off, no electrical power was needed to maintain the resistance within a given state. The distribution of the programming voltages (V_{Set} and V_{Reset}), another critical parameter to evaluate the memory device, is shown in Fig. 4(c). Figure 4(d) shows The statistical distribution of the programming voltages. As can be seen, V_{Set} and V_{Reset} distribute in a range of 0.3 V to 1 V and –0.3 V to –0.9 V, respectively. The switching threshold voltages of the Cu/GO/Pt sandwiched structure are lower than those of most reported RRAM devices (Szot et al., 2006; Tsubouchi et al., 2007; Guan et al., 2007; Fujiwara et al., 2008; Li et al., 2008).

The retention performance of the Cu/GO/Pt memory cell at room temperature is shown in Fig. 5. The device is switched On or Off by dc voltage sweeping. Then the resistance of LRS or HRS is read out at a reading voltage of 0.1 V. The reading of the resistance state is nondestructive, and no electrical power is needed to maintain the resistance within a given state (LRS or HRS). As can be seen in Fig. 5, the LRS and HRS resistances are kept stable for more than 10^4 s, indicating that the memory device is nonvolatile and stable at room temperature.

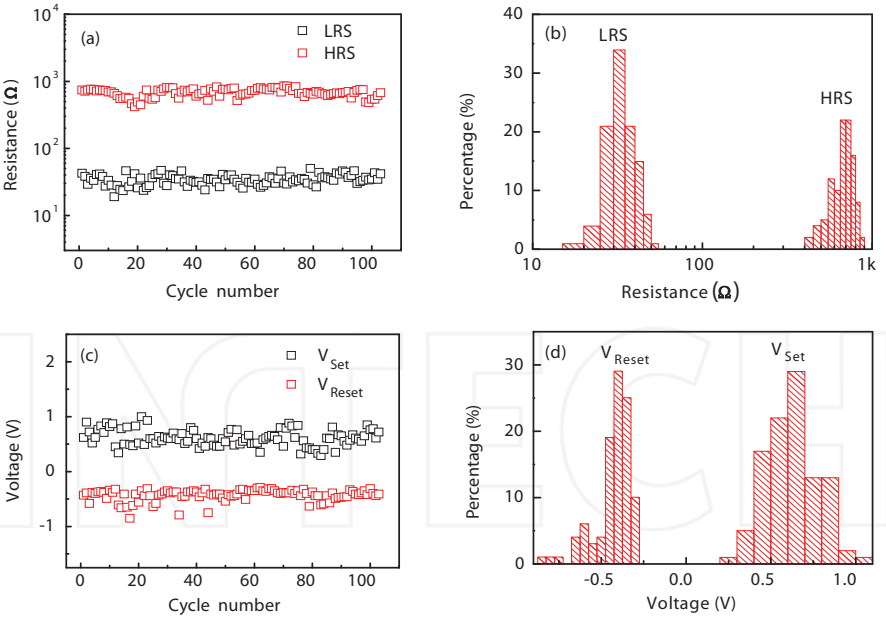

Fig. 4. (a) Endurance performance of the Cu/GO/Pt memory cell. The resistance values are read out at 0.1 V in each sweep. (b) Statistical distribution of the resistances in HRS and LRS. (c) Evolution of V_{Set} and V_{Reset} of the Cu/GO/Pt device as a function of the switching cycle. (d) Statistical distribution of V_{Set} and V_{Reset}

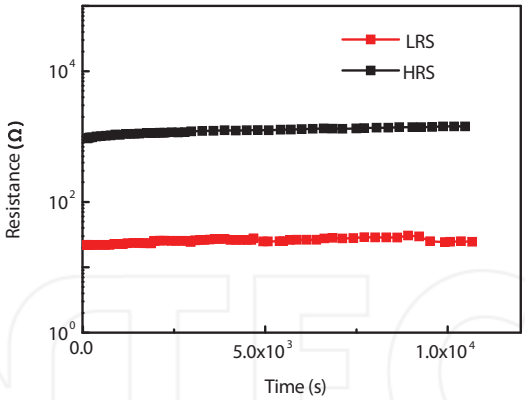

Fig. 5. Retention performance for the LRS and HRS of the Cu/GO/Pt memory cell at room temperature

To understand the conduction mechanisms of the Cu/GO/Pt memory cell, the *I-V* curves are replotted in a log-log scale. Figures 6(a) and (b) show the logarithmic plot and linear fitting of the previous *I-V* curve for the positive and negative voltage sweep regions, respectively. As shown in Fig. 6, the *I-V* curve of LRS exhibits a linearly Ohmic behavior with a slope of ~1. However, the conduction mechanisms of HRS are much more complicated. Fitting results for HRS suggest that the charge transport behavior is in good agreement with a trap-controlled space charge limited current (SCLC), which consists of two portions: the Ohmic region ($I \propto V$) and the Child's law region ($I \propto V^2$) (Strukov et al., 2008; Kim et al., 2007; Son & Shin, 2008; Chen et al., 2008). The different conduction behaviors in HRS and LRS suggest that the high conductivity in On-state cell is likely to be a confined effect rather than a homogenously distributed one (Zhuge et al., 2010).

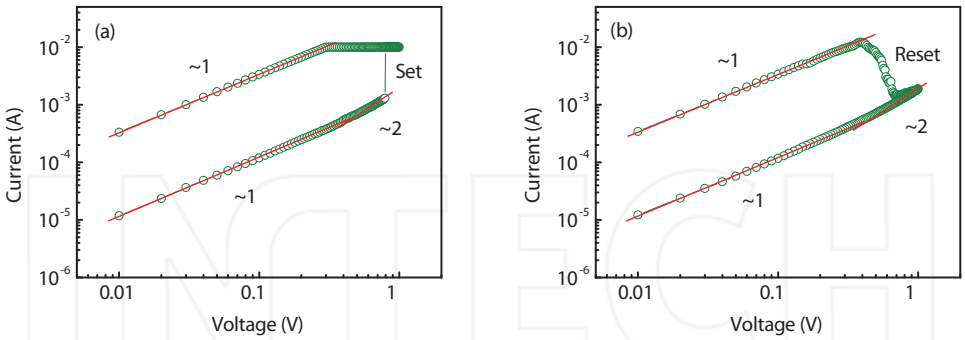

Fig. 6. *I-V* curves of the the Cu/GO/Pt memory cell plotted in log-log scale and the linear fitting results in both LRS and HRS: (a) positive voltage region and (b) negative voltage region. Also shown are the corresponding slopes for different portions

3.3 Top electrode material dependence of resistive switching of metal/GO/Pt sandwiches

Various metals (Cu, Ag, Au, and Ti) as top electrodes are deposited on GO films and the *I-V* characteristics of the corresponding metal/GO/Pt memory cells are investigated. The

similar bipolar switching behaviors are observed in these four types of metal/GO/Pt sandwiched structures. Actually, a Forming process, which is the first transition from fresh state to low resistance state, is always needed before such sandwiches show good resistive switching characteristics. However, this is not desired in practical applications because the Forming voltage is usually much higher than the Set voltage of the device. Most materials, for example, NiO, TiO_2, ZnO, CuO, and $SrTiO_3$ etc. (Kinoshita et al., 2006; Do et al., 2008; Chang et al., 2008; Fujiwara et al., 2008; Oligschlaeger et al., 2006), have already been reported to be in need of Forming process. It is necessary to find some solutions to overcome this difficulty. Kinoshita et al. developed a NiO_y film (y=0.88±0.05) free from Forming process, where a grain structure was found with conductive atomic force microscopy and most current flows through grain boundaries to obviate the requirement of Forming (Kinoshita et al., 2006). Herein, the effect of top electrode materials on the Forming process in GO thin films is investigated.

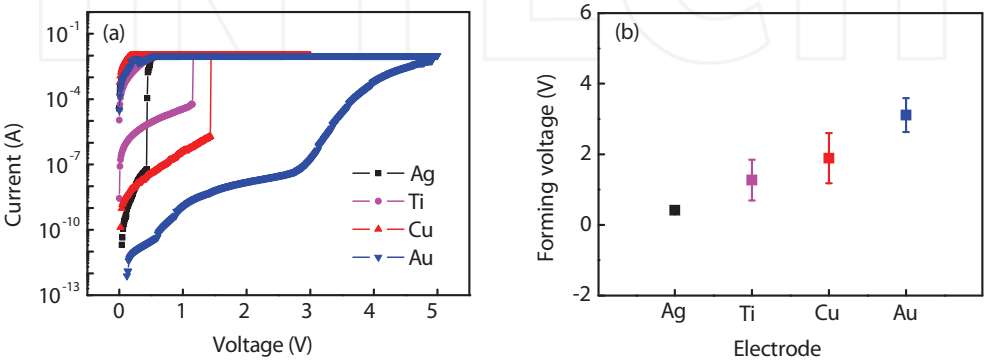

Fig. 7. (a) *I-V* curves of Forming processes of GO-based memory cells using different metals (Ag, Ti, Cu, and Au) as top electrodes. (b) Forming voltages of different metal/GO/Pt sandwiches

Figure 7(a) shows the *I-V* properties of Forming processes of Ag/GO/Pt, Ti/GO/Pt, Cu/GO/Pt, and Au/GO/Pt sandwiched structures. The Forming voltages of different metal/GO/Pt memory cells are shown in Fig. 7(b). As can be seen from Fig. 7, the Ag/GO/Pt structures have the lowest Forming voltages of about 0.4 V, while the Au/GO/Pt sandwiches show the highest Forming voltages of about 3 V. The Forming voltage of the metal/GO/Pt memory cell varies as follows: $V_{Ag}<V_{Ti}<V_{Cu}<V_{Au}$. It has been reported that solid electrolyte memory devices based on silver ions generally show low switching voltages (Kund et al., 2005; Schindler et al., 2007; Tsunoda et al., 2007). Banno et al. further clarified that the switching voltage for turn-on in RRAM devices based on solid electrolyte such as $Cu_{2-a}S$ and Ta_2O_5 could be strongly affected by the ion flux which is proportional to the product of the diffusion coefficient and the concentration of ions (Banno et al., 2008). Therefore, we can infer that a large ion diffusion coefficient can lead to a large ion flux and thus a low switching voltage. Govindaraj et al. have reported that Ag has a large diffusion coefficient in oxide films (Govindaraj et al., 2001). The Ag/ZrO_2/Au structure shows low switching voltages of <1 V without any Forming process (Li et al., 2010). In our case, it is likely that Ag also has a large diffusion coefficient in GO thin films, resulting in low Forming voltages for Ag/GO/Pt memory cells. The high Forming voltages

for Au/GO/Pt structures are likely due to gold's chemical inertness. Compared to other top electrode metals (i.e. Ag, Ti, and Cu), Gold is very difficult to be oxidized to the ions. High voltages are necessary for the activation of Au/GO/Pt memory cells.

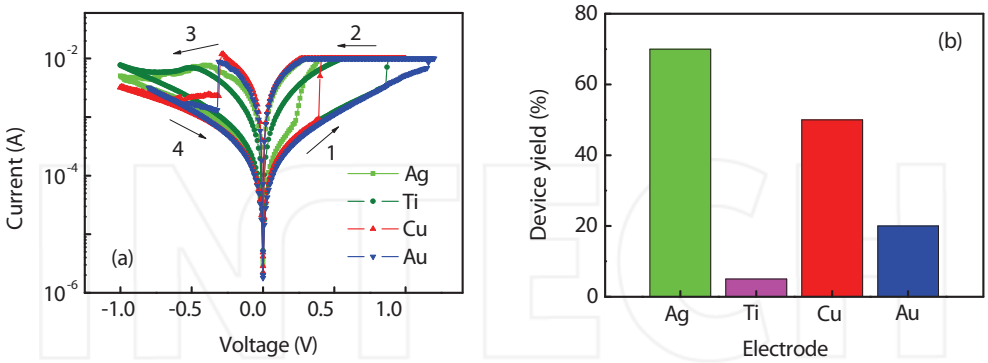

Fig. 8. (a) Typical *I-V* characteristics of GO-based memory cells using different metals (Ag, Ti, Cu, and Au) as top electrodes shown in semilogarithmic scale. (b) Device yields of different metal/GO/Pt sandwiches

Figure 8(a) shows the typical *I-V* characteristics of Ag/GO/Pt, Ti/GO/Pt, Cu/GO/Pt, and Au/GO/Pt sandwiched structures after Forming processes. Similar to the Forming processes, the Ag/GO/Pt structures have the lowest Set voltages of about 0.25 V, and the Au/GO/Pt sandwiches show the highest Set voltages of about 1.2 V. Figure 8(b) shows the top electrode dependence of device yields of metal/GO/Pt memory cells. As can be seen from Fig. 8(b), the device yield (*Y*) of the metal/GO/Pt memory cell varies as follows: $Y_{Ag}>Y_{Cu}>Y_{Au}>Y_{Ti}$. The Ag/GO/Pt structure has the highest device yield of about 70%. The strong top electrode material dependence of the switching characteristics is helpful for speculating about the resistive switching mechanism in GO thin films. It will be discussed later.

3.4 GO film thickness dependence of resistive switching of metal/GO/Pt sandwiches

Figure 9(a) shows the *I-V* characteristics of Forming processes of Cu/GO/Pt memory cells using GO films with different thicknesses, i.e. 15 nm, 30 nm, 60 nm, and 90 nm. The GO film thickness dependence of Forming voltages of Cu/GO/Pt memory cells is shown in Fig. 9(b). Obviously, the voltage required for the initial Forming process increases with the thickness of GO, indicating that the electric field inside the bulk GO is the controlling factor of the Forming. The similar experiment results have been also obtained in some oxides, for example, Fe_2O_3 (Inoue et al., 2008). Therefore, to reduce the Forming voltage or even entirely remove the Forming process of the metal/GO/Pt memory cell, an appropriate thickness of the GO thin film should be considered.

The resistances of the high resistive state and low resistive state after the Forming process for Cu/GO/Pt memory cells are shown in Fig. 10, as a function of the thickness of GO. No obvious variation can be observed for both HRS resistance and LRS resistance as the GO thickness changes from 15 nm to 90 nm. The thickness-insensitive property of HRS resistance and LRS resistance indicates that once the Forming process is completed, it is unlikely that the bulk region of GO contributes to the resistive switching effectively. This also underpins that the switching phenomenon occurs at the interface rather than the bulk region.

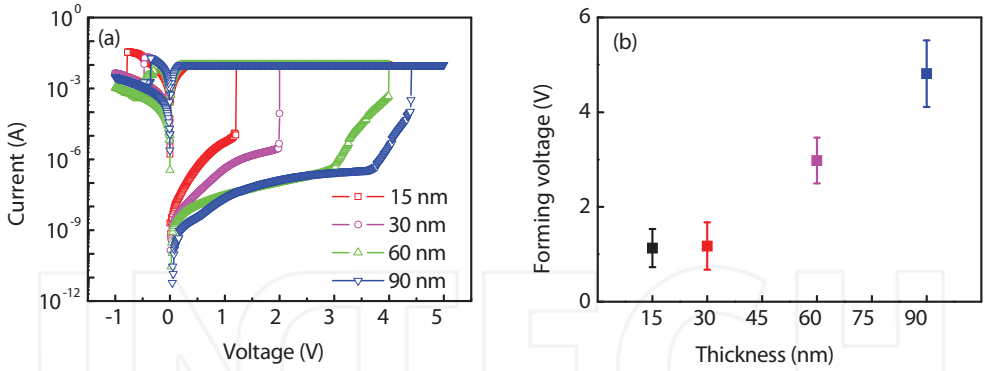

Fig. 9. (a) *I-V* curves of Forming processes of Cu/GO/Pt memory cells using GO films with different thicknesses, i.e. 15 nm, 30 nm, 60 nm, and 90 nm. (b) GO film thickness dependence of Forming voltages of Cu/GO/Pt memory cells

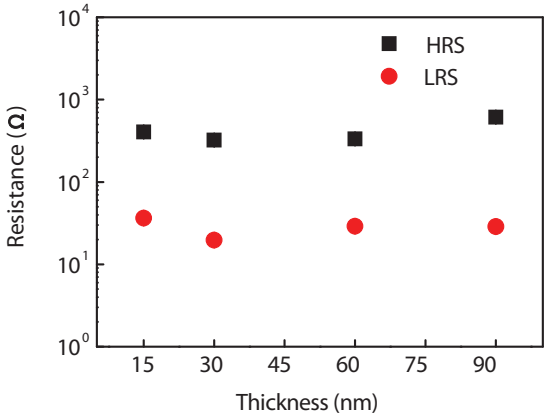

Fig. 10. Resistances of the high resistive state and low resistive state for Cu/GO/Pt memory cells, plotted against the thickness of GO

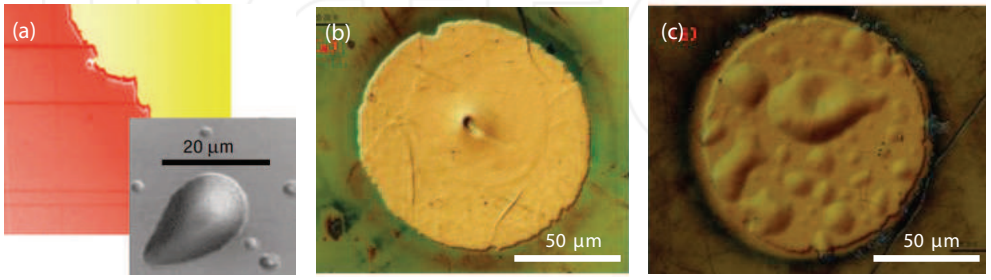

Fig. 11. Gas bubbles under the electrodes formed during the Forming processes of (a) the Pt/single crystalline $SrTiO_3$/Pt memory cell (Szot et al., 2006), (b) Cu/GO/Pt memory cell with a GO thickness of 90 nm, and (c) Au/GO/Pt memory cell with a GO thickness of 30 nm

Szot et al. investigated the resistive switching of the Pt/single crystalline $SrTiO_3$/Pt memory cell and found gas bubbles under the anode. This phenomenon was explained by the polyfilamentary models proposed in the context of amorphous-oxide films (Dearnaley et al., 1970; Rakhshani et al., 1976; Ray et al., 1990), namely the preferential diffusion of oxygen and solid-state electrolytic processes along a discrete set of filaments, which give rise to a located decomposition and subsequent accumulation of oxygen gas under the anode. In our case, such gas bubbles are also observed under the top electrodes for the Cu/GO/Pt memory cell with a GO thickness of 90 nm and Au/GO/Pt memory cell with a GO thickness of 30 nm. From Fig. 7, we see that for the Au/GO/Pt cell, the Forming voltage is more than 4 V. As can be seen from Fig. 9, the Cu/GO/Pt cell with a GO thickness of 90 nm needs a high Forming voltage of about 5V. Therefore, we infer that as the high Forming voltage is applied to the GO-based memory cell, a large amount of heat is generated in a confined region, resulting in an increase of temperature. Then, the high temperature in the confined region may cause the decomposition of epoxide, hydroxyl, and/or carboxyl groups in GO, resulting in water steam and CO_2 (Zhou et al., 2006).

3.5 Current compliance dependence of resistive switching of metal/GO/Pt sandwiches

A current compliance is usually needed during the Forming and Set processes to prevent the sample from a permanent breakdown. We find that the current compliance is another critical parameter to determine the resistive switching characteristics of metal/GO/Pt memory cells. Figure 12(a) shows the typical *I-V* characteristics of the Au/GO/Pt device with different current compliance (0.02 A, 0.04 A, and 0.07 A). Clearly, the Reset current (maximum current level before the Reset process) increases with increasing compliance current. As mentioned above, the different conduction behaviors in high and low resistance states suggest that the high conductivity in On-state cell is likely to be a confined effect rather than a homogenously distributed one. It is likely due to the formation of conducting filaments in GO (Yang et al., 2009). It is considered that stronger filaments with a higher density are formed at a larger current compliance (Rohde et al., 2005). The Reset process is also considered to be due to the rupture of the filaments due to the heat generated by the large current flow (Rohde et al., 2005). Thus, it can be imagined that a larger Reset current is necessary for the Reset process at the larger current compliance. The dependence of the Reset current and resistance in the low resistance state on current compliance applied in the Set process is shown in Fig. 12(b). We see that the Reset current has an approximate linear relationship to the current compliance. Thus, the power needed for the WRITE and ERASE operations in RRAM can be modulated by controlling the current compliance. As can be seen from Fig. 12(b), the resistance in the low resistance state decreases with increasing current compliance. Therefore, different resistance states can be achieved using different current compliances in the program process, showing good potential for multilevel storage (Wang et al., 2010). Figure 12(c) shows the current compliance dependence of the Set and Reset voltages. The Set voltage shows weak dependence on current compliance, whereas the Reset voltage increases obviously with increasing current compliance applied in the Set process.

3.6 Possible mechanisms of resistive switching in GO thin films

i. Filamentary model for metal/GO/Pt sandwiches

As mentioned above, the strong top electrode material dependence of the switching characteristics is helpful for speculating about the resistive switching mechanism in GO thin

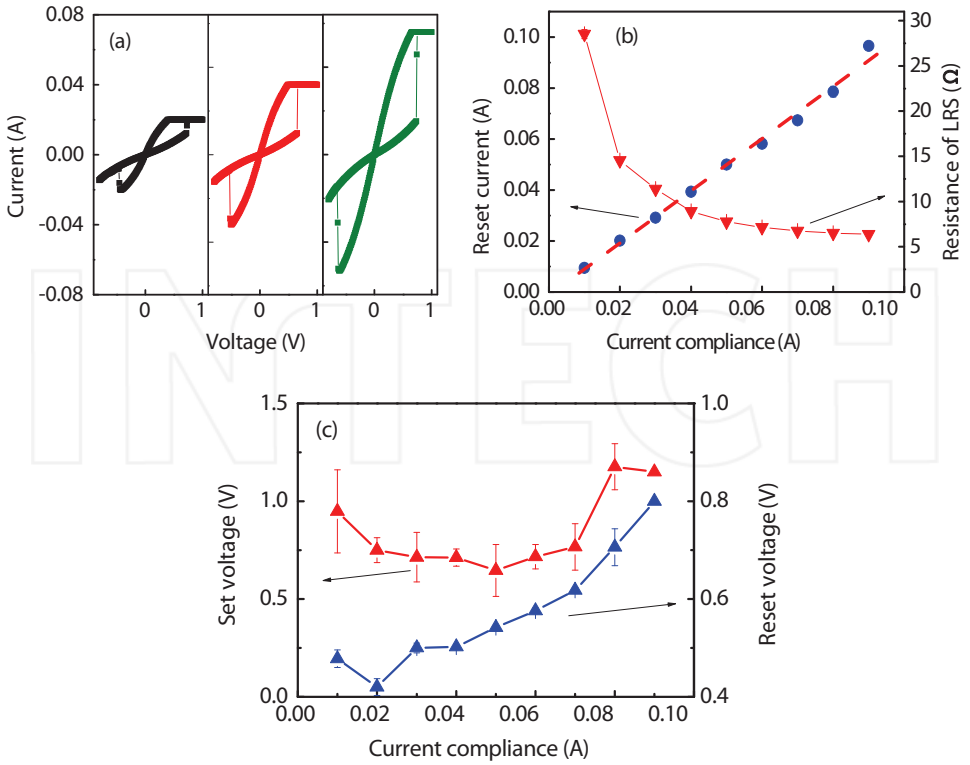

Fig. 12. (a) Typical *I-V* characteristics of the Au/GO/Pt device with different current compliance (0.02 A, 0.04 A, and 0.07 A). (b) Current compliance dependence of the Reset current and resistance of the low resistance state of the Au/GO/Pt device. (c) Current compliance dependence of the Set and Reset voltages of the Au/GO/Pt device.

films. Tokunaga et al. investigated the RS effect at the interface between metal electrodes (Pt, Au, Ag, Al, Ti, and Mg) and atomically flat cleaved (001) surfaces of $La_{1-x}Sr_{1+x}MnO_4$ (x=0−1.0) single crystals (Tokunaga et al., 2006). Hysteretic *I-V* characteristics were observed in the junctions for Mg, Al, and Ti, which have relatively shallow work functions (Φ). In our case, Ti, Cu, and Ag have a lower Φ of 3.98 eV, 4.35 eV, and 4.26 eV, respectively, whereas Au has a higher one of 5.1 eV. It indicates that the occurrence of the resistive switching in metal/GO/Pt structures is irrelevant to Φ of the top electrodes. Liao and co-workers studied the resistive switching characteristics of metal/$Pr_{0.7}Ca_{0.3}MnO_3$ (PCMO)/Pt devices and found that devices with top electrode made of Al, Ti, and Ta exhibit a bipolar resistive switching, but those with top electrode made of Pt, Ag, Au, and Cu do not (Liao et al., 2009). The resistive switching was attributed to a thin metal-oxide layer formed at the interface between the former group of top electrode and PCMO. In our work, the top electrode material includes both reactive metals such as Ti and inert metals such as Au. Therefore, the observed resistive switching is not due to the formation of a metal-oxide layer at the interface between the top electrode and GO. The strong top electrode material dependence of the resistive switching characteristics of GO thin films suggests that the resistive

switching effect may be attributed to the formation/rupture of metal filaments due to the diffusion of the top electrodes under a bias voltage. Briefly, a positive voltage (>V_{Set}) on the top electrodes generates a high electric field that drives metal (e.g., Ag) ions into the GO matrix and form conducting filaments inside the GO layer, and the device reaches the On state. After the Set process, the device retains the On state unless a sufficient voltage of opposite polarity (<V_{Reset}) is applied and the electrochemical dissolution of the metal filaments Resets the device, and the Off state is finally reached again (Jo et al., 2008; Zhuge et al., 2010).

To verify the physical nature of the resistive switching effect of the metal/GO/Pt structures, resistances in the low and high resistance states of the Cu/GO/Pt device are measured as a function of temperature. Figure 13(a) shows the typical metallic behavior of the resistance in the On state. In contrast, the resistance in the Off state shows a semiconducting behavior as displayed in the inset of Fig. 13(a). The metallic conducting behavior in the low resistance state indicates the formation of conducting filaments in the GO films. The temperature dependence of metallic resistance can be written as $R(T) = R_0[1 + a(T - T_0)]$, where R_0 is the resistance at temperature T_0, and a is the temperature coefficient of resistance. By choosing T_0 as 300 K, the temperature coefficient of resistance of the filaments is calculated to be 1.7×10^{-3} K^{-1}, which is similar to the value 2.5×10^{-3} K^{-1} for high-purity copper nanowires of diameter ≥15 nm (Bid et al., 2006), confirming that the filaments are composed of Cu in metallic states due to the diffusion of the top electrode under a bias voltage. The discrepancy of the temperature coefficient of resistance is attributed to inevitable defects in the Cu filaments, since the presence of defects can reduce the temperature coefficient of resistance by shortening the mean free path of electrons (Bid et al., 2006).

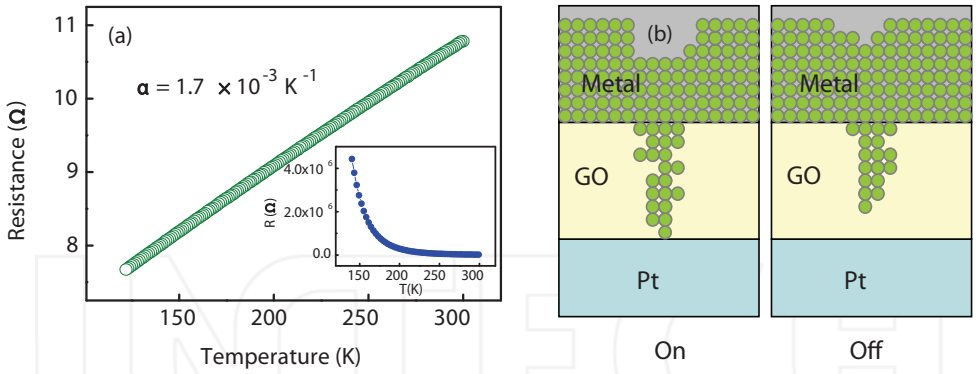

Fig. 13. (a) Temperature dependence of the resistance in the low resistance sate of the Cu/GO/Pt device. The inset shows the temperature dependence of the resistance in the high resistance state. Also shown is the temperature coefficient of resistance (a) of the conducting filaments. (b) A schematic diagram for the mechanism of resistive switching effects in metal/GO/Pt devices.

ii. Desorption/absorption of oxygen-related group on the GO sheets

Figure 14(a) shows the typical local *I-V* characteristics of GO films by the conductive atomic force microscopy measurements in which the AFM tip is in perpetual contact with the sample. The obvious bipolar resistive switching effect is also observed though the threshold

voltages are higher probably due to the nonideal contact between the AFM probe and GO films as well as very small contact area compared to the conventional *I-V* characterization (Yin et al., 2010). In this case, we intend to attribute the observed resistive switching to the desorption/absorption of oxygen-related groups on the GO sheets. As shown in Fig. 14(c), a GO layer can be considered as a graphene sheet with epoxide, hydroxyl, and/or carboxyl groups attached to both sides, and physical properties of GO can be modulated by those chemical functionalities on the surface (Yan et al., 2009). When there are an amount of epoxide, hydroxyl, and carboxyl groups on the GO surface, the conductance of GO is assumed to be low due to sp^3 bonding feature. As a negative voltage bias is applied on the bottom electrode (i.e., Pt), some oxygen-related functional groups inside the GO layers are removed, resulting in an amount of sp^2 bonds. The conductance of GO becomes higher due to an increase in the concentration of interlayer π electrons. As a result, the sample is switched to the low resistance state (On state). While sweeping the voltage to certain positive values, the oxygen-related groups diffuse toward GO sheets and attach to them again. Correspondingly, the sample returns to the high resistance state (Off state). Therefore, as schematically shown in Fig. 14(b), the desorption and absorption of the oxygen-related functional groups on the GO sheets correspond to the low and high resistive states, respectively.

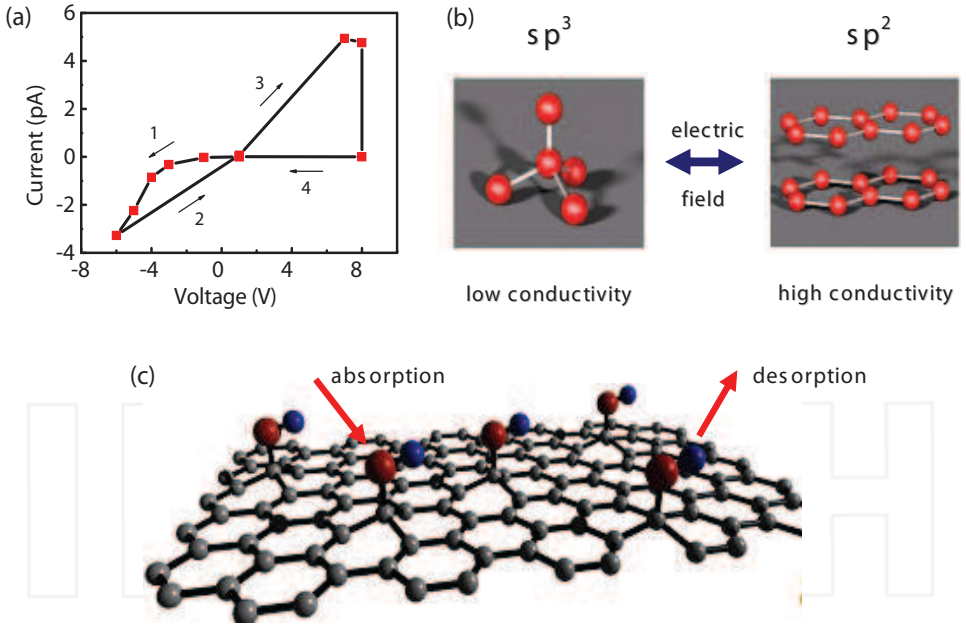

Fig. 14. (a) Typical local *I-V* characteristics of GO films measured by conductive atomic force microscopy. The voltage is swept in the direction as follows: 0 V → –6 V → 0 V → 8 V → 0 V. (b) Insulating carbon can be switched to conductive sp^2-rich carbon and conductive carbon can be switched to sp^3-rich carbon by applying appropriate electric fields (Kreupl et al., 2008). (c) Schematic of the desorption and aborption of hydroxyl or similar groups on the GO sheets (Echtermeyer et al., 2008).

4. Conclusion

Reliable and reproducible resistive switching behaviors are observed in GO thin films. The metal/GO/Pt structures exhibit an On/Off ratio of about 20, switching threshold voltages of less than 1 V, good retention and endurance performances. The Ag/GO/Pt structure has a low Forming voltage likely due to a large Ag ion diffusion coefficient in GO, whereas the Au/GO/Pt structure shows a high Forming voltage likely due to gold's chemical inertness. The Forming voltage increases with the thickness of GO, indicating that the electric field inside the bulk GO is the controlling factor of the Forming. The resistances of the high and low resistance states show weak dependence on the film thickness, demonstrating that the resistive switching occurs in a confined region. It is found that the resistance of the On state decreases with current compliance, whereas the Reset current and Reset voltage increase with current compliance. Therefore, by adjusting current compliance, the power consumption of RRAM can be modulated and multilevel storage can be realized. The resistive switching is also observed in micro-regions by conducting atomic force microscope. The dominant conduction mechanisms of low and high resistance states are Ohmic behavior and trap-controlled space charge limited current, respectively. Based on the experimental results, the possible physical mechanisms of resistive switching behaviors in GO thin films can be understood by considering the desorption/absorption of oxygen-related groups on the GO sheets as well as the formation/rupture of conducting filaments.

This work was supported by State Key Research Program of China (973 Program), National Natural Science Foundation of China, Zhejiang and Ningbo Natural Science Foundations, Chinese Academy of Sciences (CAS), Zhejiang Qianjiang Talent Project, and State Key Lab of Silicon Materials (China).

5. References

*Corresponding author. Electronic mail: runweili@nimte.ac.cn.

Avouris P.; Chen Z. H.; & Perebeinos V. (2007). Carbon-based electronics. *Nature Nanotechnology*, Vol. 2, No. 10, 605-615, ISSN: 1748-3387

Banno N.; Sakamoto T.; Iguchi N.; Sunamura H.; Terabe K.; Hasegawa T. & Aono M. (2008). Diffusivity of Cu ions in solid electrolyte and its effect on the performance of nanometer-scale switch. *IEEE Transactions on Electron Devices*, Vol. 55, No. 11, 3283–3287, ISSN: 0018-9383

Beck A.; Bednorz J. G.; Gerber Ch.; Rosse C.L. & Widmer D. (2000). Reproducible switching effect in thin oxide films for memory applications. *Applied Physics Letters*, Vol. 77, No. 1, 139-141, ISSN: 0003-6951

Bid A.; Bora A. & Raychaudhuri A. (2006). Temperature dependence of the resistance of metallic nanowires of diameter ≥15 nm: Applicability of Bloch-Gruneisen theorem. Physical Review B, Vol. 74, No. 3, 035426, ISSN: 1098-0121

Burghard M.; Klauk H.; & Kern K. (2009). Carbon-Based Field-Effect Transistors for Nanoelectronics. *Advanced Materials*. Vol. 21, No. 25-26, 2586-2600, ISSN: 0935-9648

Chang W. Y.; Lai Y. C.; Wu T. B.; Wang S. F.; Chen F. & Tsai M. J. (2008). Unipolar resistive switching characteristics of ZnO thin films for nonvolatile memory applications. *Applied Physics Letters*. Vol. 92, No. 2,022110, ISSN: 0003-6951

Chen X. M.; Wu G. H. & Bao D. H. (2008). Resistive switching behavior of Pt/$Mg_{0.2}Zn_{0.8}O$/Pt devices for nonvolatile memory applications. *Applied Physics Letters*, Vol. 93, No. 9, 093501, ISSN: 0003-6951

Cote L. J.; Kim F. & Huang J. X. (2009). Langmuir−Blodgett Assembly of Graphite Oxide Single Layers. *Journal of the American Chemical Society,* Vol. 131, No. 3, 1043-1049, ISSN: 0002-7863

Dearnaley, G.; Morgan, D. V. & Stoneham, A. M. (1970). A model for filament growth and switching in amorphous oxide films. *Journal of Non-Crystalline Solids,* Vol. 4, 593–612, ISSN: 0022-3093

Dearnaley, G.; Stoneham, A. M. & Morgan, D. V. (1970). Electrical phenomena in amorphous oxide films. *Reports on Progress in Physics,* Vol. 33, No. 3, 1129–1191, ISSN: 0034-4885

Do Y. H.; Kwak J. S.; Hong J. P.; Jung K. & Im H. (2008). Al electrode dependent transition to bipolar resistive switching characteristics in pure TiO_2 films. *Journal of Applied physics*, Vol. 104, No. 11, 114512, ISSN: 0021-8979

Dong Y.; Yu, M G.; McAlpine C.; Lu W. & Lieber C. M. (2008). Si/α-Si core/shell nanowires as nonvolatile crossbar switches. *Nano Letters*, Vol. 8, No. 2, 386-391, ISSN: 1530-6984

Echtermeyer T. J.; Lemme M. C.; M. Baus et al. (2007). A grapheme-based electrochemical switch. arXiv:0712.2026v1

Eda G.; Fanchini G. & Chhowalla M. (2008). Large-area ultrathin films of reduced graphene oxide as a transparent and flexible electronic material. *Nature Nanotechnology*, Vol. 3, No. 5, 270-274, ISSN: 1748-3387

Fujiwara K.; Nemoto T.; Rozenberg M. J.; Nakamura Y. & Takagi H. (2008). Resistance Switching and Formation of a Conductive Bridge in Metal/Binary Oxide/Metal Structure for Memory Devices. *Japanese Journal of Applied Physics*, Vol. 47, No. 8, 6266-6271, ISSN: 0021-4922

Govindaraj R.; Kesavamoorthy R.; Mythili R. & Viswanathan B. (2001). The formation and characterization of silver clusters in zirconia. *Journal of Applied Physics*, Vol. 90, No. 2, 958–963, ISSN : 0021-4922

Guan W. H.; Long S. B.; Jia R.& Liu M. (2007). Nonvolatile resistive switching memory utilizing gold nanocrystals embedded in zirconium oxide. *Applied Physics Letters,* Vol. 91, No. 6, 062111, ISSN: 0003-6951

Guan W. H.; Liu M.; Long S. B.; Liu Q. & Wang W. (2008). On the resistive switching mechanisms of Cu/ZrO_2:Cu/Pt. *Applied Physics Letters* , Vol. 93, No. 22, 223506, ISSN: 0003-6951

He C. L.; Zhuge F.; Zhou X. F.; Li M.; Zhou G. C.; Liu Y. W.; Wang J. Z.; Chen B.; Su W. J.; Liu Z. P.; Wu Y. H.; Cui P. & Li R. W. (2009). Nonvolatile resistive switching in grapheme oxide thin films. *Applied Physics Letters*, Vol. 95, No. 23, 232101, ISSN: 0003-6951

Hummers W. S. & Offeman R. E. (1958). Preparation of Graphitic Oxide. *Journal of the American Chemical Society,* Vol. 80, No. 6,1339, ISSN: 0002-7863

Inoue I. H.; Yasuda S.; Akinaga H. & Takagi H. (2008). Nonpolar resistance switching of metal/binary-transition-metal oxides/metal sandwiches: Homogeneous/inhomogeneous transtion of current distribution. *Physical Review B*, Vol. 77, No. 3, 035105, ISSN: 1098-0121

Jeong D. S.; Schroeder H. & Waser R. (2009). Abnormal bipolar-like resistance change behavior induced by symmetric electroforming in Pt/TiO_2/Pt resistive switching cells. *Nanotechnology*, Vol. 20, No. 37, 375201, ISSN: 0957-4484

Jo S. H. & Lu W. (2008). CMOS Compatible Nanoscale Nonvolatile Resistance Switching Memory. *Nano Letters,* Vol. 8, No. 2, 392-397, ISSN: 1476-1122

Jo S. H.; Kim K. H. & Lu W. (2009). Programmable Resistance Switching in Nanoscale Two-Terminal Devices. *Nano Letters*, Vol. 9, No. 1, 496-500, ISSN: 1476-1122

Jo, S. H.; Kim K. H. & Lu W. (2009). High-Density Crossbar Arrays Based on a Si Memristive System. *Nano Letters*, Vol. 9, No. 2, 870-874 , ISSN: 1476-1122

Kim D. C.; Lee M. J.; Ahn S. E.; Seo S.; Park J. C.; Yoo I. K.; Baek I. G.; Kim H. J.; Yim E. K.; Lee J. E.; Park S. O.; Kim H. S.; In Chung U.; Moon J. T. & Ryu B. I. (2006). Improvement of resistive memory switching in NiO using IrO_2. *Applied Physics Letters*, Vol. 88, No. 23, 232106, ISSN: 0003-6951

Kim K. M.; Choi B. J.; Shin Y. C.; Choi S. & Hwang C. S. (2007). Anode-interface localized filamentary mechanism in resistive switching of TiO_2 thin films. *Applied Physics Letters*, Vol. 91, No. 1, 012907, ISSN: 0003-6951

Kim S.; Moon H.; Gupta D.; Yoo S. & Choi Y. K. (2009). Resistive Switching Characteristics of Sol–Gel Zinc Oxide Films for Flexible Memory Applications. *IEEE Transactions on Electron Devices*, Vol. 56, No. 4, 696-699 , ISSN: 0018-9383

Kinoshita K.; Tamura T.; Aoki M.; Sugiyama Y. & Tanaka H. (2006). Bias polarity dependent data retention of resistive random access memory consisting of binary transition metal oxide. *Applied Physics Letters*, Vol. 89, No. 10, 103509, ISSN: 0003-6951

Kinoshita K.; Yoshida C.; Aso H.; Aoki M. & Sugiyama Y. (2006). Thermal properties of NiO_y resistor practically free from the "forming" process, *Proceedings of International Conference on Solid State Devices and Materials*, pp. 570-571, Pacifico Yokohama Yokohama, Japan, Sept. 2006

Kreupl F.; Bruchhaus R.; Majewski P. et al. (2008). Carbon-based resistive memory. *Proceeding of IEEE Electron Devices Meeting*, pp. 521-524

Kund M.; Beitel G.; Pinnow C.U.; Röhr T.; Schumann J.; Symanczyk R.; Ufert K.D. & Müller G. (2005). Conductive bridging RAM (CBRAM): An emerging non-volatile memory technology scalable to sub 20 nm, *Electron Devices Meeting, 2005, IEDM Technical Digest, IEEE International*, pp. 754–757. ISBN: 0-7803-9268-x, Washington, DC, Dec. 2005, IEEE

Kwon D. H.; Kim K. M.; Jang J. H.; Jeon J. M.; Lee M. H.; Kim G. H.; Li X. S.; Park G. S.; Lee B.; Han S.; Kim M. & Hwang C. S. (2010). Atomic structure of conducting nanofilaments in TiO_2 resistive switching memory. *Nature Nanotechnology*, Vol. 5, No. 2, 148-153, ISSN: 1748-3387

Lee M. J.; Park Y.; Suh D. S.; Lee E. H.; Seo S.; Kim D. C.; Jung R.; Kang B. S.; Ahn S. E.; Lee C. B.; Seo D. H.; Cha Y. K.; Yoo I. K.; Kim, J. S. & Park B. H. (2007). Two Series Oxide Resistors Applicable to High Speed and High Density Nonvolatile Memory. *Advanced Materials*, Vol. 19, No. 22, 3919-3923, ISSN: 0935-9648

Li Y. B.; Sintskii A. & Tour J. M. (2008). Electronic two-terminal bistable graphitic memories. *Nature Materials*, Vol. 7, No. 12, 966 -971, ISSN: 1476-1122

Li M.; Zhuge F.; Zhu X. J.; Yin K. B.; Wang J. Z.; Liu Y. W.; He C. L.; Chen B. & Li R. W. (2010). Nonvolatile resistive switching in metal/La-doped $BiFeO_3$/Pt sandwiches. *Nanotechnology*, Vol. 21, No. 42, 425202, ISSN: 0957-4484

Li Y. T.; Long S. B.; Zhang M. H.; Liu Q.; Shao L. B.; Zhang S.; Wang Y.; Zuo Q. Y.; Liu S. & Liu M. (2010). Resistive switching properties of Au/ZrO_2/Ag structure for low-voltage nonvolatile memory applications. *IEEE Electron Device Letters*, Vol. 31, No. 2, 117-119, ISSN: 0741-3106

Liao Z. L.; Wang Z. Z.; Meng Y.; Liu Z. Y.; Gao P.; Gang J. L.; Zhao H. W.; Liang X. J.; Bai X. D. & Chen D. M. (2009). Categorization of resistive switching of metal-$Pr_{0.7}Ca_{0.3}MnO_3$-metal devices. *Applied Physics Letters*, Vol. 94, No. 25, 253503, ISSN: 0003-6951

Liu S. Q.; Wu N. J. & Ignatiev A. (2000). Electric-pulse-induced reversible resistance change effect in magnetoresistive films. *Applied Physics Letters*, Vol. 76, No. 19, 2749-2751, ISSN: 0003-695

Liu Q.; Long S. B.; Wang W.; Zuo Q. Y.; Zhang S.; Chen J. N. & Liu M. (2009). Improvement of Resistive Switching Properties in ZrO_2 -Based ReRAM With Implanted Ti Ions. *IEEE Electron Device Letters,* Vol. 30, No. 12, 1335-1337, ISSN: 0741-3106

Lu W. & Lieber C. M. (2007). Nanoelectronics from the bottom up. *Nature Materials*, Vol. 6, No. 11, 841-850, ISSN: 1476-1122

Meijer G. I. (2008). MATERIALS SCIENCE: Who Wins the Nonvolatile Memory Race?. *Science*, Vol. 319, No. 5870, 1625-1626, ISSN: 0036-8075

Novoselov K. S.; Geim A. K.; Morozov S. V.; Jiang D.; Zhang Y.; Dubonos S. V.; Grigorieva I. V.; & Firsov A. A. (2004). Electric field effect in atomically thin carbon films. *Science*, Vol. 306, No. 5696, 666-669, ISSN: 0036-8075

Odagawa A.; Sato H.; Inoue, I. H.; Akoh H.; Kawasaki M.& Tokura Y. (2004). Colossal electroresistance of a $Pr_{0.7}Ca_{0.3}MnO_3$ thin film at room temperature. *Physical Review B*, Vol. 70, No. 22, 224403, ISSN: 1098-0121

Oligschlaeger R.; Waser R.; Meyer R.; Karthauser S. & Dittmann R. (2006). Resistive switching and data reliability of epitaxial (Ba,Sr)TiO_3 thin films. *Applied Physics Letters*, Vol. 88, No. 4, 042901, ISSN: 0003-6951

Rakhshani, A. E.; Hogarth, C. A. & Abidi, A. A. (1976). Observations of local defects caused by electrical conduction through thin sandwich structures of Ag–SiO/BaO–Ag. *Journal of Non-Crystalline Solids,* Vol. 20, No. 1, 25–42, ISSN: 0022-3093

Ray, A. K. & Hogarth, C. A. (1990). Recent advances in the polyfilamentary model for electronic conduction in electro-formed insulating films. *International Journal of Electronics,* Vol. 69, No. 1, 97–107, ISSN: 0020-7217

Rohde C.; Choi B. J.; Jeong D. S.; Choi S.; Zhao J. S. & Hwang C. S. (2005). Identification of a determining parameter for resistive switching of TiO_2 thin films. *Applied Physics Letters*, Vol. 86, No. 26, 262907, ISSN: 0003-6951

Rueckes T.; Kim K.; Joselevich E.; Tseng G. Y.; Cheung C. L.; & Lieber C. M. (2000). Carbon nanotube-based nonvolatile random access memory for molecular computing. *Science*, Vol. 289, No. 5476, 94-97, ISSN: 0036-8075

Schindler C.; Meier M. & Waser R. (2007). Resistive switching in Ag-Ge-Se with extremely low write currents, *Proceedings of Non-Volatile Memory Technology Symposium*, pp. 82–85, Print ISBN: 978-1-4244-1361-4, Albuquerque, NM, Nov. 2007, IEEE

Seo S.; Lee M. J.; Seo D. H.; Jeoung E. J.; Suh D.S.; Joung Y. S.; Yoo I. K.; Hwang I. R.; Kim S. H.; Byun I. S.; Kim J.S.; Choi J. S. & Park B. H. (2004). Reproducible resistance switching in polycrystalline NiO films. *Applied Physics Letters*, Vol. 85, No. 23, 5655-5657, ISSN: 0003-6951

Son J. Y. & Shin Y. H. (2008). Direct observation of conducting filaments on resistive switching of NiO thin films. *Applied Physics Letters*, Vol. 92, No. 22, 222106, ISSN: 0003-6951

Stewart D. R.; Ohlberg D. A. A.; Beck P. A.; Chen Y.; Williams R. S.; Jeppesen J. O.; Nielsen K. A. & Stoddart J. F. (2004). Molecule-Independent Electrical Switching in Pt/Organic Monolayer/Ti Devices. *Nano Letters*, Vol. 4, No. 1, 133-136, ISSN: 1476-1122

Strukov D. B.; Snider G. S.; Stewart D. R. & Williams R. S. (2008). The missing memristor found. *Nature*, Vol. 453, No. 7191, 80 -83, ISSN: 0028-0836

Szot K.; Speier W.; Bihlmayer G. & Waser R. (2006). Switching the electrical resistance of individual dislocations in single-crystalline $SrTiO_3$. *Nature Materials* , Vol. 5, No. 4, 312-320, ISSN: 1476-1122

Tokunaga Y.; Kaneko Y.; He J. P.; Arima T.; Sawa A.; Fuji T.; Kawasaki M. et al. (2006). Colossal electroresistance effect at metal electrode/$La_{1-x}Sr_{1+x}MnO_4$ interfaces. *Applied Physics Letters,* Vol. 88, No. 22, 223507, ISSN: 0003-6951

Tsubouchi K.; Ohkubo I.; Kumigashira H.; Oshima M.; Matsumoto Y.; Itaka K.; Ohnishi T. et al. (2007). High-Throughput Characterization of Metal Electrode Performance for Electric-Field-Induced Resistance Switching in Metal/$Pr_{0.7}Ca_{0.3}MnO_3$/Metal Structures. *Advanced Materials*, Vol. 19, No. 13, 1711-1713, ISSN: 1476-1122

Tsunoda K.; Fukuzumi Y.; Jameson J. R.; Wang Z.; Griffin P. B. & Nishi Y. (2007). Bipolar resistive switching in polycrystalline TiO2 films. *Applied Physics Letters,* Vol. 90, No. 11, 113501, ISSN: 0003-6951

Wang X. R.; Ouyang Y. J.; Li X. L.; Wang H. L.; Guo J.; & Dai H. J. (2008). Room-Temperature All-Semiconducting Sub-10-nm Graphene Nanoribbon Field-Effect Transistors. *Physical Review Letters,* Vol. 100, No. 20, 206803, ISSN: 0031-9007

Waser R. & Aono M. (2007). Nanoionics-based resistive switching memories. *Nature Materials*, Vol. 6, No. 11, 833-840, ISSN: 1476-1122

Wu X.; Zhou P.; Li J; Chen, L. Y.; Lv H. B.; Lin Y. Y. & Tang T. A. (2007). Reproducible unipolar resistance switching in stoichiometric ZrO_2 films. *Applied Physics Letters*, Vol. 90, No. 18 ,183507, ISSN: 0003-6951

Yan J. A.; Xian L. & Chou M. Y. (2009). Structural and electronic properties of oxidized graphene, *Physical Review Letters*, Vol. 103, No. 8, 086802, ISSN: 0031-9007

Yang C. H.; Seidel J.; Kim S. Y.; Rossen P. B.; Yu P.; Gajek M.; Chu Y. H.; Martin L. W.; Holcomb M. B.; He Q.; Maksymovych P.; Balke N.; Kalinin S. V.; Baddorf A. P.; Basu S. R. et al. (2009). Electric modulation of conduction in multiferroic Ca-doped $BiFeO_3$ films. *Nature Materials*, Vol. 8, No. 6, 485-493, ISSN: 1476-1122

Yang Y. C.; Pan F.; Liu Q.; Liu M. & Zeng F. (2009). Fully Room-Temperature-Fabricated Nonvolatile Resistive Memory for Ultrafast and High-Density Memory Application. *Nano Letters*, Vol. 9, No. 4, 1636-1643, ISSN: 1476-1122

Yin K. B.; Li M.; Liu Y. W.; He C. L.; Zhuge F.; Chen B.; Lu W.; Pan X. Q. & Li R. W. (2010). Resistance switching in polycrystalline $BiFeO_3$ thin films. *Applied Physics Letters,* Vol. 97, No. 4, 042101, ISSN: 0003-6951

Zhou X. F. & Liu Z. P. (2010). A Scalable, Solution-phase Processing Route to Ultralarge Graphene Sheets. *Chemical Communications*, Vol. 46, No. 15, 2611-2613, ISSN: 1359-7345

Zhou Y. H.; Liu H. B.; Fu L.; Li B. & Chen Z. Z. (2006). Influence of pyrolytic temperature on structures and properties of graphite oxide. *Journal of the Chinese Ceramic Society*, Vol. 34, No. 3, 318-323, ISSN: 0454-5648

Zhuge F.; Dai W.; He C. L.; Wang A. Y.; Liu Y. W.; Li M.; Wu Y. H.; Cui P. & Li R. W. (2010). Nonvolatile resistive switching memory based on amorphous carbon. *Applied Physics Letters*, Vol. 96, No. 16,163505, ISSN: 0003-6951

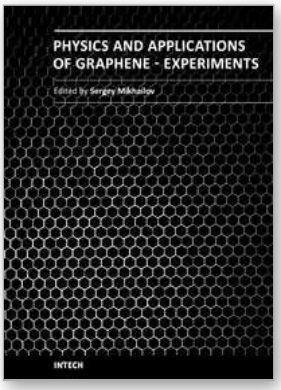

Physics and Applications of Graphene - Experiments

Edited by Dr. Sergey Mikhailov

ISBN 978-953-307-217-3
Hard cover, 540 pages
Publisher InTech
Published online 19, April, 2011
Published in print edition April, 2011

The Stone Age, the Bronze Age, the Iron Age... Every global epoch in the history of the mankind is characterized by materials used in it. In 2004 a new era in material science was opened: the era of graphene or, more generally, of two-dimensional materials. Graphene is the strongest and the most stretchable known material, it has the record thermal conductivity and the very high mobility of charge carriers. It demonstrates many interesting fundamental physical effects and promises a lot of applications, among which are conductive ink, terahertz transistors, ultrafast photodetectors and bendable touch screens. In 2010 Andre Geim and Konstantin Novoselov were awarded the Nobel Prize in Physics "for groundbreaking experiments regarding the two-dimensional material graphene". The two volumes Physics and Applications of Graphene - Experiments and Physics and Applications of Graphene - Theory contain a collection of research articles reporting on different aspects of experimental and theoretical studies of this new material.

INTECH
open science | open minds

InTech Europe
University Campus STeP Ri
Slavka Krautzeka 83/A
51000 Rijeka, Croatia
Phone: +385 (51) 770 447
Fax: +385 (51) 686 166
www.intechopen.com

InTech China
Unit 405, Office Block, Hotel Equatorial Shanghai
No.65, Yan An Road (West), Shanghai, 200040, China
中国上海市延安西路65号上海国际贵都大饭店办公楼405单元
Phone: +86-21-62489820
Fax: +86-21-62489821